National Physical Laboratory

NPL REPORT IR 46

REPORT ON DOSE MEASUREMENTS ON THE MRI-LINAC AT LIVERPOOL HOSPITAL (AUSTRALIA) PERFORMED BY NPL

ILIAS BILLAS, MICHAEL HOMER AND SIMON DUANE

JANUARY 2018

Department for Business, Energy & Industrial Strategy

FUNDED BY BEIS

Report on dose measurements on the MRI-linac at Liverpool Hospital (Australia) performed by NPL

Ilias Billas, Michael Homer and Simon Duane
Chemical Medical and Enviro Science

ABSTRACT

This report describes measurements of the radiation dose from the MRI-linac at Liverpool Hospital (Australia) using a selection of detectors (such as ionisation chambers, alanine and Gafchromic EBT-3 films) in order to calibrate the machine output. Absorbed dose to water calibration coefficients for the ionisation chambers used in the constant magnetic field (1 T) of the MRI-Linac machine were also measured. Together with similar measurements performed at NPL in a 0 T magnetic field over a range of beam qualities, the corrections required to measure the absorbed dose in the presence of a magnetic field using these detectors was determined.

ISSN 1754-2952

National Physical Laboratory
Hampton Road, Teddington, Middlesex, TW11 0LW

Approved on behalf of NPLML by
Dr Giuseppe Schettino, Science Area Leader

CONTENTS

1 INTRODUCTION

MRI-guided radiotherapy (MRIgRT), a state-of-the-art cancer treatment, combines a linear accelerator (linac) with a Magnetic Resonance Imaging (MRI) scanner. An MRI-linac provides real-time images during a patient's treatment and greatly enhanced soft-tissue image contrast, while completely avoiding the radiation dose associated with X-ray systems. MRIgRT is expected to improve real-time adaptive planning based on high-contrast moving visual images on the change of the tumour characteristics and explore the possibilities of an advanced personalised radiotherapy.

While great benefits for cancer treatment are anticipated using this new technology, there are, however, issues that need to be addressed. Among them is the effect of the external magnetic field (B-field) on the dose distribution in water and dosimeters. Although the photon beam is not affected by the B-field, the direction of motion of the secondary electrons is changed (known as electron return effect, ERE). The affected trajectories of these electrons is known to modify ion chamber sensitivity and the absorbed dose distribution in water (Raaijmakers *et al.*, 2005, Raaijmakers *et al.*, 2007, Raaymakers *et al.*, 2004, O'Brien *et al.*, 2016).

Measurements and Monte Carlo (MC) calculations have previously been made to characterise the response of different types of ionisation chambers (Meijsing *et al.*, 2009, Smit *et al.*, 2013, O'Brien *et al.*, 2016, Reynolds *et al.*, 2013, Spindeldreier *et al.*, 2017). These works investigated the optimal chamber orientation with respect to the B-field and radiation beam, parallel (||) or perpendicular (⊥), as well as the B-field correction factors at different field strengths. Considering the change in the chamber response relative to a B-field strength of 0 T, these studies found that when the ionisation chamber axis is:

- (⊥) to the B-field and the radiation beam is (⊥) to B-field, the change is ranging from 4% - 11.3%.
- (||) to the B-field and the radiation beam is (⊥) to B-field, the change is <1%.
- (||) or (⊥) to the B-field and the radiation beam is (||) to the B-field, the change is <1% for a B-field strength up to 1 T and increases to approximately 2% at 1.5 T.

The B-field correction factor (which is explained in section 3.9), for different types of ionisation chambers, is ranging from 0.992 to 1.005 when the chamber is parallel to the B-field and 0.953 to 0.976 when the chamber is perpendicular to the B-field.

The aim of this work was to make measurements using both an Ion Beam Applications (IBA) and a Physikalisch-Technische Werkstätten (PTW) Farmer-type chamber, a PTW Roos chamber, a PTW Semiflex 3D chamber, Gafchromic EBT-3 film and alanine/EPR dosimeters (Electron Paramagnetic Resonance), as a first step in determining correction factors and the optimum setup for Farmer-type chamber-based dosimetry in the MRI-linac at Liverpool Hospital, Australia (throughout the rest of the report referred to as 'Australian MRI-linac'). The measurements involved determining beam output as well as calibration coefficients, by substitution, for each of the ionisation chambers. More information regarding the Australian MRI-linac program can be found in literature (Keall *et al.*, 2014, Liney *et al.*, 2016).

The change in sensitivity of an air-filled ion chamber due to the ERE in a 1 T B-field depends on the chamber cavity size and shape and is expected to vary with chamber type. A study by Gallas *et al* (Gallas, 2017) investigated the change in the sensitivity of alanine due to the ERE by varying the air gap around the alanine pellets inside the pellet holder. They found that the ERE does not affect the dose readout of alanine.

The EPR readout signal from an alanine dosimeter is proportional to the number of stable free radicals resulting from previous irradiation of the alanine. Strong B-fields can be expected to modify diffusion and recombination of ions in irradiated alanine and so the free radical yield may be sensitive to the B-field strength at the time of irradiation. The sensitivity of alanine in terms of absorbed dose to water as a function of B-field strength has been measured at the United Kingdom National Physical Laboratory

(NPL) over a range from 0 T to 2 T, using a General Motors Worldwide (GMW) type 3474-140 electromagnet at two different beam qualities (^{60}Co and 8 MV linac beam). Results have shown that the strong B-field in an MRI-linac has a measureable but small effect on the sensitivity of alanine in terms of absorbed dose to water. A B-field correction factor of 0.997 (for 1 T B-field strength) has been applied to all alanine dose measurements. This correction was determined by interpolating the Australian MRI-linac beam quality to the ^{60}Co and 8 MV beam qualities.

The alanine dosimetry system, both Farmer-type ionisation chambers and one of the PTW Roos ionisation chambers (NPL-owned) used in this investigation have been calibrated at NPL. The calibration was performed in zero B-field strength, for a range of megavoltage X-Ray beams between 4 MV and 18 MV, and in ^{60}Co radiation, traceable to the NPL reference standard of absorbed dose to water. One of the IBA Farmer-type chambers (owned by the Liverpool Cancer Therapy Centre, Australia) was also calibrated in energies between 4 MV and 10 MV without a conventional beam flattening filter.

Alanine has a weak beam quality dependence in its sensitivity, and produces a slightly smaller signal for a given dose when irradiated by megavoltage X-rays compared to ^{60}Co radiation. A correction factor of 1.004 has been included in all the alanine dose measurements reported here.

2 MATERIAL AND METHODS

Measurements were made in the MRI-linac facility at Liverpool Hospital Australia and in a conventional linac at NPL (zero B-field strength).

Absorbed dose was measured per Gy delivered so far (one GSF is nominally equal to 1 Gy at 1 m from the target):

- at the isocentre
- in a static horizontal beam (gantry angle = 90^{o}), with the detector axis perpendicular to the beam and also to the B-field (figure 1).
- in a field size of approximately 10 cm x 10 cm at the measurement plane
- in a water tank (Medtec MT-DDA s/n: 973, 40 cm x 39 cm x 32 cm.)
- in a water-equivalent full-scatter phantom (30 cm x 30 cm), assembled from two different manufactures:
    - ‘RMI’ solid water: 9 cm and 19 cm used for build-up and a 2 cm plate with the dosimeters located in the mid-plane
    - ‘Gammex’ solid water: 10 cm used for backscatter.
- at a water-equivalent depth of 10 cm and 20 cm

The monitor chamber was an Exradin type A1SL ion chamber (NPL-owned) and the following dosimeters were used:

- PTW waterproof Farmer-type chamber (type 30013)
- IBA waterproof Famer-type chamber (type FC65-G)
- PTW Semiflex 3D chamber (type 31021)
- PTW Roos chamber (type 34001)
- Gafchromic EBT-3 film
- Alanine (seven of 5 mm diameter and 2.5 mm thick pellets in a waterproof Farmer-shaped polyether ether ketone (PEEK) holder)

Each dosimeter is located in its own holder in the water tank. For solid water, Farmer-type chambers only and alanine were placed in the 2 cm insert and films were stuck to the surface of a 1 cm thick solid water plate.

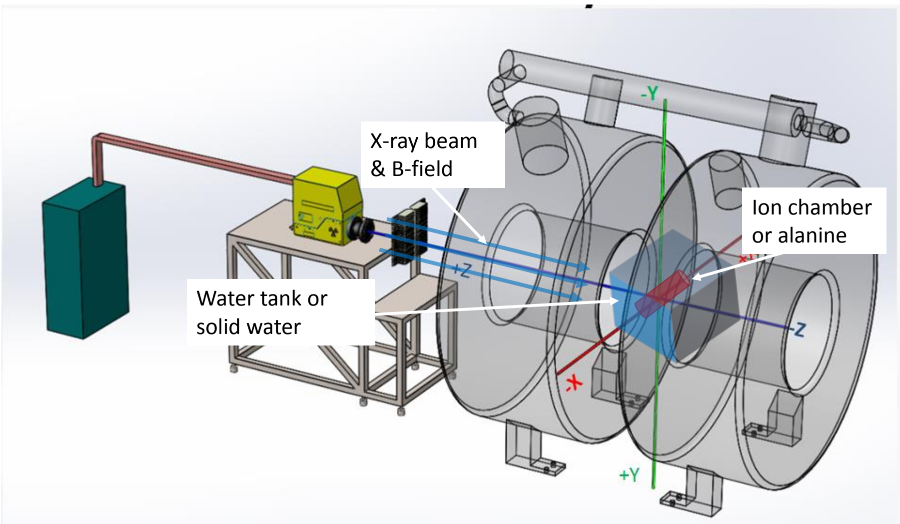

Figure 1. X-ray beam, B-field and ion chamber/alanine orientation (Figure adopted with permission from Jarrad Begg, Liverpool Hospital, Australia).

2.1 SET UP IN THE MRI-LINAC (1 T B-FIELD)

Measurements were performed using a water tank and a solid water phantom (figure 2) and were mounted on a fixed bench, used to support the measurement equipment between the two bores of the MRI-linac.

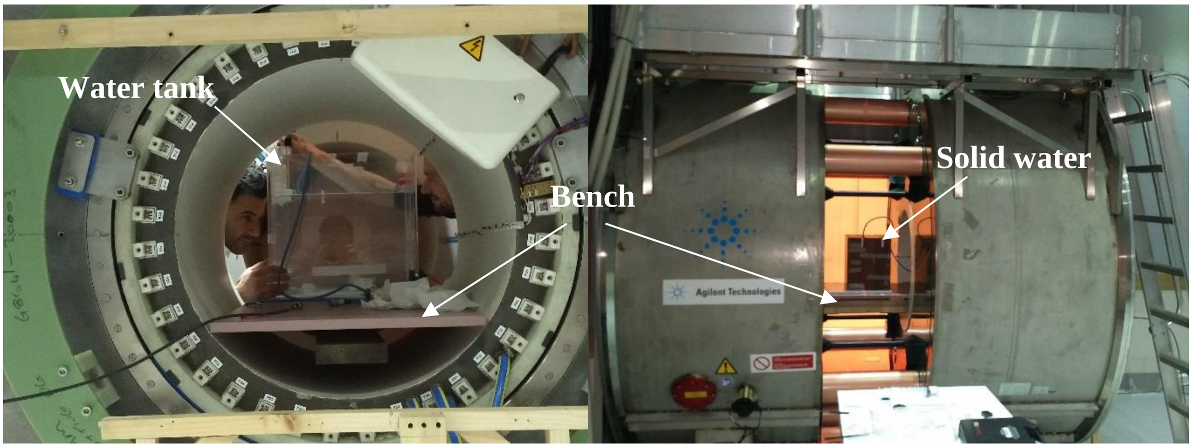

Figure 2. Water tank (left) and solid water (right) experimental setup.

2.1.1 Water tank setup

The water tank was provided by Liverpool Hospital and had dimensions of 40 cm width, 39 cm height and 32 cm depth. A polymethyl methacrylate (PMMA) holder that could accommodate the detectors was fixed to a manual stepping mechanism enabling the crossline movement. Fixed PMMA rods (machined at NPL) were used to set up the detectors in the inline position at a water-equivalent depth of 10 cm and 20 cm.

2.1.2 Solid water setup

The solid water consisted of 10 cm of water-equivalent plate sheets stacked at the back of a 2 cm thick plate with a Farmer-shaped cavity. Alanine dosimeters and Farmer-type chambers were positioned within the solid water plate at a depth of 1 cm of solid water. The solid water plates were assembled such that:

- at least 10 cm water-equivalent backscatter material was at the back of the 2 cm thick plate with a Farmer-shaped cavity

- the solid water plates were positioned so that the dosimeter measurement point was at the required source-to-chamber distance (SCD)
- a combination of solid water plates put the dosimeter measurement point at the required depth. For instance, with 9 cm solid water in front of the 2 cm thick plate with a Farmer-shaped cavity, the measurement point of the alanine dosimeter and Farmer-type chambers is 10 cm from the front surface.

2.2 BEAM OUTPUT

Output measurements were performed using alanine dosimeters in a water tank and in a solid water phantom at a water-equivalent depth of 10 cm (the geometric centre of the measuring detector was set up at a depth of 10 cm from the front surface). Both the radiation beam and the B-field were orientated horizontally along the central axis of the two bores (inline orientation so that the radiation beam is aligned with the B-field) and the phantom was positioned such that the longitudinal axis of alanine detectors was perpendicular to both the beam and the B-field (figure 1).

Following local practice, both the water tank and the solid water were set up to an isocentre indicated by the three wall-mounted room lasers and had a distance of 2.84 m from the target. The water tank and the solid water were aligned and located so that the reference point of the detector would coincide with the indicated isocentre.

An Exradin A1SL ionisation chamber was used as an external monitor. The chamber was connected to a Standard Imaging Supermax electrometer (Channel 1) on the first measurement day (26 June 2017) and on a local Fluke electrometer (s/n: 99789) for the rest of the days due to failure of the Supermax's channel 1. The chamber was operated at 300 V polarising potential to collect a negative ionisation charge. The monitor chamber was present for all measurements.

Ambient air pressure was measured in the control room and temperature was measured with a mercury thermometer placed in the water tank and in the solid water plate with a Farmer-shaped cavity. A Digitron (s/n: 12) thermometer was placed in close proximity to the external monitor chamber.
The local mercury thermometer was cross-checked with the NPL calibrated Digitron (s/n: 12) thermometer. It was found that a deviation of 0.2 ºC had to be added to the final reading of the temperature.

Gy so far (GSF) is the calibrated unit of the linac at 1 m. One GSF is nominally equal to 1 Gy at 1 m from the target.

The field size was defined by the leaves of the multi-leaf collimator (MLC) and was nominally 10 cm x 10 cm at the isocentre (actual: 8.7 cm x 10 cm). Another relevant machine parameter is a dose rate of approximetly 7.1 GSF/minute. The majority of ionisation chamber measurements were with beam deliveries of 10 GSF, and alanine measurements were with beam deliveries of 231 GSF.

2.3 ION RECOMBINATION

An ionisation chamber reading must have a correction applied for the incomplete collection of charge due to ion recombination, k_{ion}. By assuming that the ion recombination is less than 3%, the two voltage method (equation 1) is a good approximation to determine k_{ion}. So, ion recombination is defined as:

$$k_{ion} - 1 = \frac{(M_1/M_2) - 1}{(V_1/V_2) - 1} \quad (1)$$

where M_1 and M_2 are the collected charges at the polarising voltages V_1 and V_2, respectively. Ion recombination for the different chamber types were determined from measurements using the water tank.

2.4 $TPR_{20/10}$ MEASUREMENT

A Tissue Phantom Ratio ($TPR_{20/10}$) measurement was performed using the water-proof Farmer-type chamber (30013/s/n: 03981) for both setups (water tank and solid water).

The ionisation chamber collected charge in a beam delivery of 10 GSF at a fixed source-to-chamber distance. The thickness of water or solid phantom in front of the chamber was either 10 cm or 20 cm and the ratio of readings at each depth was taken. In solid water setup the 10 cm of material was composed of 9 cm of RMI solid water and the 1 cm of the front of the Farmer-shaped cavity plate. The 20 cm of material had 10 cm of RMI solid water in addition to the 10 cm of material described previously, with 10 cm of Gammex solid water providing backscatter in both configurations.

2.5 DOSE AS A FUNCTION OF POSITION FOR ALANINE

The dose per GSF and dose per external monitor signal (Exter.Mon.) delivered to each alanine pellet in a Farmer-type holder was investigated as a function of position within the holder.

2.6 AIR GAP EEFECT ON THE SOLID WATER SETUP

Measurements were performed with a Farmer chamber set up in the 2 cm air cavity of the solid water. In one case the air cavity was filled with water and in the other case it was left empty.

2.7 FILM IRRADIATIONS

2.7.1 Film response curve

Films were manipulated, processed and analysed by using the method developed by Bouchard *et al.* (2009). Briefly, twelve pieces of EBT3 films (3.5 cm x 3.5 cm) were positioned in the solid water. The source-to-surface distance was set at 2.84 m and films were irradiated at a depth of 10 cm with10 cm solid water used to provide backscatter. The maximum given dose was approximately 10 Gy. The film response curve was expressed in netOD as a function of dose where netOD is the difference between the optical density (OD) of an irradiated film and the OD of an un-irradiated film.

2.7.2 Application films

Four sets of application films were irradiated at the same setup as the film response curve. Each set consisted of four film pieces from the same sheet with dimensions of 5 cm x 7 cm. Each film piece was irradiated with a dose of approximately 3.5 Gy.

2.7.3 Film digitisation

The films were digitised with an EPSON Expression 10000XL Pro flat-bed colour scanner in transmission mode. Coloured images were acquired at a spatial resolution of 150 dpi with 48 bit RGB and all scanner colour corrections turned off. A frame was used to position the films at an area of the scanner bed which could correct films for scanner light non-uniformity (Saur and Frengen, 2008). The orientation of all films were kept constant and aligned within $\pm 5^{o}$ to avoid any effect due to polarised light. A 3.5 mm PMMA sheet was placed on top of the films during digitisation in order to position the films flat on the scanner bed. The scanner warming-up effect was diminished by using ten repeated scans. Films were scanned before, to account for background correction, and 5 to 6 days after irradiation.

2.8 MEASUREMENTS AT NPL

The Liverpool Cancer Centre’s IBA Farmer-type chamber was brought to the National Physical Laboratory in Teddington and calibrated in terms of absorbed dose to water in the NPL Elekta Synergy linac. The calibration was performed against the reference standards for absorbed dose to water, in both flattened and flattening filter-free beams, and is traceable to the UK primary standard of absorbed dose for photon beams. NPL certificates 2017RD01819-1R and 2017RD01819-2 were produced from these measurements.

2.9 MAGNETIC FIELD CORRECTION FACTOR

The B-field correction factor, k_Q^B, corrects for the effects of the difference between the reference condition (no B-field) and the actual user condition (with B-field). For the determination of k_Q^B we could use the analogy of the beam quality correction factor, k_{Q,Q_0}. This is explained further in this section.
The reference measurement of the absorbed dose is determined by the detector's response, M, and the application of the calibration coefficient in terms of absorbed dose to water, $N_{D,w}$, under the reference conditions used in the standards laboratory.

$$D_w = M\, N_{D,w}$$

In most clinical situations the measurement conditions do not match the reference conditions used at the standards laboratories. Usually, dosimeters are used in a different energy beam from that used at a standards laboratory (which is typically ^{60}Co). In order to measure the dose to water in the user beam quality, Q, the effect of the difference between the reference beam quality Q_0 and the actual user quality Q needs to be corrected for. This can be achieved by applying a beam quality correction factor (k_{Q,Q_0}).

$$D_{w,Q} = M_Q\, k_{Q,Q_0}\, N_{D,w,Q_0}$$

The correction factor k_{Q,Q_0} is defined as the ratio of the calibration coefficient that you want, $N_{D,w,Q}$, divided by the calibration coefficient that you have, N_{D,w,Q_0}.

$$k_{Q,Q_0} \equiv \frac{N_{D,w,Q}}{N_{D,w,Q_0}}$$

Similarly, the B-field correction factor, k_Q^B, is defined as the ratio of the calibration coefficient that you want, $N_{D,w,Q}^B$, divided by the calibration coefficient that you have, $N_{D,w,Q}$.

$$k_Q^B \equiv \frac{N_{D,w,Q}^B}{N_{D,w,Q}}$$

The absorbed dose to water, measured under the influence of a particular B-field, is the product of the measured signal from the detector used in that B-field and the detector's calibration coefficient for that B-field (which can be determined at a primary standards laboratory).

$$D_{w,Q}^B = M_Q^B\, N_{D,w,Q}^B$$

However, if the calibration coefficient is applicable to a B-field of 0 T, then k_Q^B could be used to determine the absorbed dose to water for B-fields greater than 0 T.

$$D_{w,Q}^B = M_Q^B\, k_Q^B\, N_{D,w,Q}$$

In the current study, alanine dosimetry was used as a reference detector to determine $N_{D,w,Q}^B$ for a variety of ion chambers in the Australian MRI-linac.

3 RESULTS

3.1 $TPR_{20/10}$ MEASUREMENT

A $TPR_{20/10}$ was determined using the water-proof Farmer-type ionisation chamber (type 30013, s/n: 03981). The values were found to be 0.647 and 0.642 for the water tank and solid water setup, respectively.

3.2 MRI-LINAC BEAM OUTPUT

Alanine dosimeters were used to calibrate the MRI-linac output on four consecutive days (26 to 29 June 2017) on both the water tank and the solid water setup. This was determined in terms of Gy/GSF and Gy/Exter.Mon. (where 'Exter.Mon.' is the corrected signal from the A1SL chamber acting as an independent monitor). The dose per alanine pellet was read out using EPR spectroscopy on return to NPL and a B-field correction factor was applied to get the absorbed dose to water at 1 T B-field strength. Table 1 shows results of the MRI-linac beam output measured with the water tank setup at each day and the average of all days. Table 2 shows results for the solid water setup. In the same table, the standard deviation (SD) and the standard deviation of the mean (SDOM) are also presented. SDOM is defined as:

$$\mathrm{SDOM}\ (\%) = \frac{\sigma_{n-1}}{\bar{x} \cdot \sqrt{n}} \cdot 100$$

Where:

σ_{n-1} is the standard deviation of n readings
$\bar{x}$ is the mean of n readings and
n is the number of readings

Table 1. Water tank setup. The MRI-linac output as measured from alanine dosimeters at three different days.

	Gy/GSF		Gy/Extr. Mon	
	Average	SDOM (%)	Average	SDOM (%)
Day 1	0.0876	0.14	0.0105	0.13
Day 2	0.0884	0.20	0.0105	0.10
Day 4	0.0901	0.03	0.0105	0.02
All days	0.0888	0.44	0.0105	0.09

Table 2. Solid water setup. The MRI-linac output as measured from alanine dosimeters for two days.

	Gy/GSF		Gy/Extr. Mon	
	Average	SDOM (%)	Average	SDOM (%)
Day 3 & 4	0.0891	0.44	0.0105	0.20

3.3 MRI-LINAC REPEATABILITY

The stability and setup repeatability of the Australian MRI-Linac are presented in figure 3, which shows the signal of the external monitor detector, the field detector (PTW Farmer chamber, s/n: 03981) and the ratio between the field and the monitor detectors over the period of 3 days. Data are normalised to the average of the signals of all days. The statistical analysis is shown in table 3.

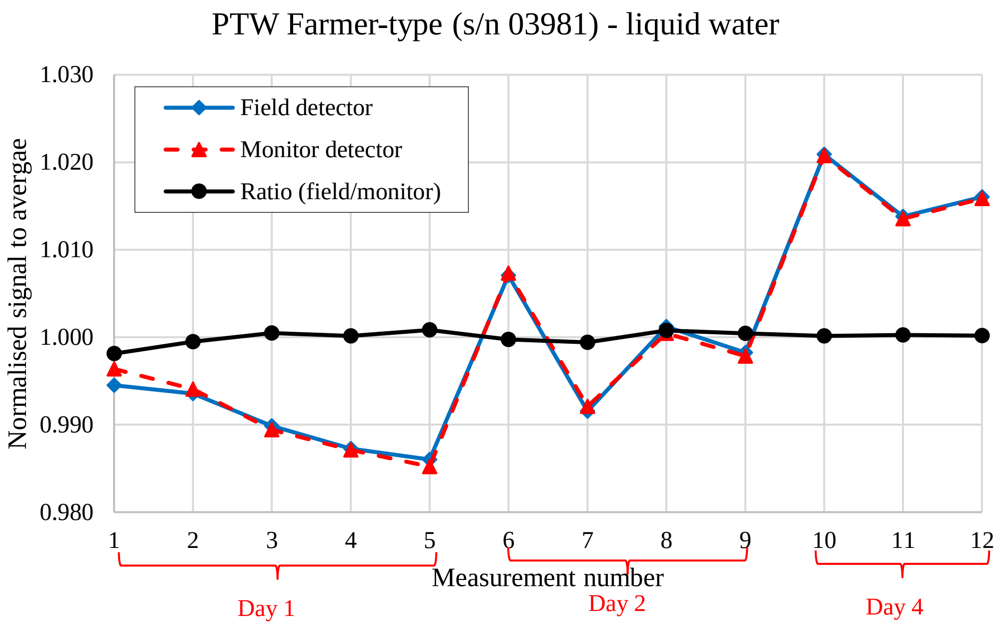

Figure 3. Normalised chamber signal over 3 days.

Table 3. Statistical analysis of MRI-Linac stability and setup repeatability

	Gy/GSF		**Gy/Extr. Mon**	
	Average	SDOM (%)	Average	SDOM (%)
Day 1	1.6487	0.17	0.1994	0.05
Day 2	1.6641	0.32	0.1999	0.03
Day 4	1.6931	0.21	0.1999	0.00
All days	1.6649	0.34	0.1997	0.04

3.4 ION RECOMBINATION

Table 4 shows the ion recombination of the four ionisation chambers.

Table 4. Ion recombination of 4 ionisation chambers

Chamber type and serial number	k_{ion}
PTW Farmer-type (s/n 03981)	1.0013
IBA Farmer-type (s/n 3520)	1.0017
IBA Farmer-type(s/n 819)	1.0012
PTW Semiflex 3D (s/n 141563)	1.0018
PTW Roos (s/n: 01394)	1.0021
PTW Roos (s/n: 01684)	1.0022

3.5 CALIBRATION BY SUBSTITUTION

The alanine measurements from the Australian MRI-linac were used to calibrate each of the ionisation chambers by the method of substitution.

Ionisation chamber calibration coefficients (Gy/C) in terms of absorbed dose to water derived from measurements performed at the Australian MRI-linac are shown in tables 5, 6, 7 and 8. Table 5 and 6 show results for the water tank setup and table 7 and 8 for the solid water setup. Alanine pellets were used as reference detectors and were corrected for the effect of the B-field at 1 T (correction of 0.997). The calibration coefficients were obtained as the ratio of dose to water measured using alanine and the corrected chamber reading. The results are relative to the MRI-linac monitor chamber (tables 5 and 7) and the external monitor chamber (tables 6 and 8) for a beam delivery of 10 GSF and 83 nC, respectively.

Table 5. Water tank setup. Summary of ionisation chamber calibration coefficients (Gy/C) in terms of absorbed dose to water as measured in the Australian MRI-linac using machine monitor unit (GSF).

Chamber type and s/n	Day 1	Day 2	Day 4	Weighted average
PTW Farmer-type (s/n: 03981)	5.313E+07	5.308E+07	5.320E+07	5.313E+07
IBA Farmer-type (s/n: 3520)	4.723E+07	4.740E+07	-	4.734E+07
IBA Farmer-type (s/n: 819)	4.699E+07	4.731E+07	-	4.723E+07
PTW Semiflex 3D (s/n: 141563)	-	-	5.811E+08	5.811E+08
PTW Roos (s/n: 01394)	-	-	8.233E+07	8.233E+07
PTW Roos (s/n: 01684)	-	-	8.270E+06	8.270E+06

Table 6. Water tank setup. Summary of ionisation chamber calibration coefficients (Gy/C) in terms of absorbed dose to water as measured in the Australian MRI-linac using an external monitor chamber.

Chamber typeand s/n	Day 1	Day 2	Day 4	Weighted average
PTW Farmer-type (s/n:03981)	5.263E+07	5.261E+07	5.267E+07	5.263E+07
IBA Farmer-type (s/n:3520)	4.676E+07	4.681E+07	-	4.679E+07
IBA Farmer-type (s/n: 819)	4.671E+07	4.683E+07	-	4.680E+07
PTW Semiflex 3D(s/n:141563)	-	-	5.769E+08	5.769E+08
PTW Roos (s/n:01394)	-	-	8.162E+07	8.162E+07
PTW Roos (s/n: 01684)	-	-	8.154E+07	8.154E+07

Table 7. Solid water setup. Summary of ionisation chamber calibration coefficients (Gy/C) in terms of absorbed dose to water as measured in the Australian MRI-linac using machine monitor unit (GSF).

Chamber type/s/n	Day 3	Day 4	Weighted average
PTW Farmer-type (s/n: 03981)	5.344E+07	5.375E+07	5.350E+07
IBA Farmer-type (s/n: 3520)	4.724E+07	-	4.724E+07
IBA Farmer-type (s/n: 819)	4.747E+07	-	4.747E+07

Table 8. Solid water setup. Summary of ionisation chamber calibration coefficients (Gy/C) in terms of absorbed dose to water as measured in the Australian MRI-linac using an external monitor chamber.

Chamber type/s/n	Day 3	Day 4	Weighted average
PTW Farmer-type (s/n: 03981)	5.283E+07	5.260E+07	5.279E+07
IBA Farmer-type (s/n: 3520)	4.695E+07	-	4.695E+07
IBA Farmer-type (s/n: 819)	4.694E+07	-	4.694E+07

3.6 AIR GAP EEFECT ON THE SOLID WATER SETUP

Table 9 shows the ratio between the field chamber and monitor chamber when the air cavity of the solid water is either filled with water or not.

Table 9. Air gap effect on the solid water setup

	field/reference	SDOM (%)
Cavity filled with water	0.223	0.023
Cavity without water	0.222	0.012
ratio (without/with)	0.997	0.03

3.7 DOSE DELIVERED TO ALANINE AS A FUNCTION OF POSITION

The dose delivered to each alanine pellet in the F-type holder was measured at NPL. The pellets were labelled 1 – 5 with 1 being closest to the stem of the alanine holder. Figures 4a and 4b show results of the MRI-linac output for each individual pellet in Gy/GSF and Gy/Exter. Mon., respectively.

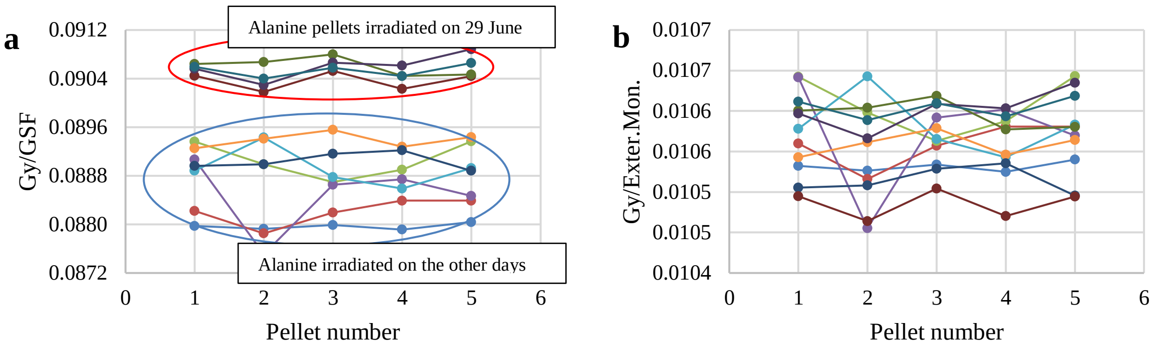

Figure 4. The beam output in terms of Gy/GSF (a) and Gy/Exter.Mon. (b) as a function of alanine pellet position within an F-type holder.

3.8 FILM ANALYSIS

The 12-point film response curve, expressed in netOD as a function of dose, is shown in figure 5.

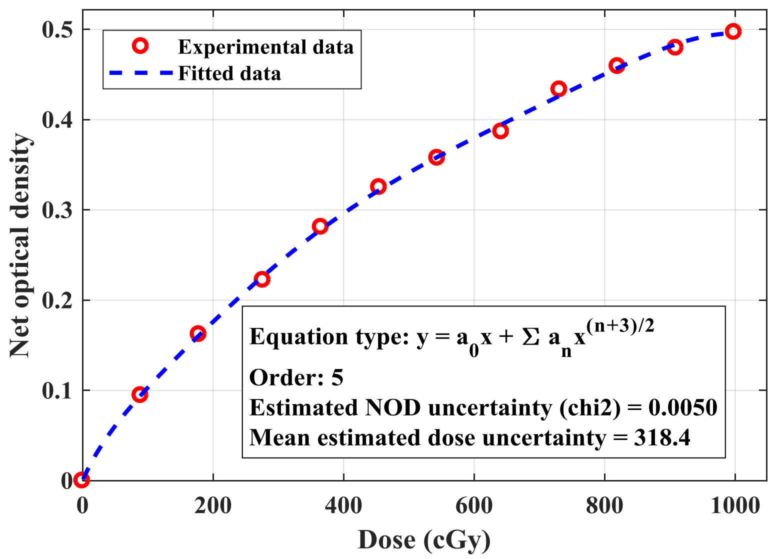

Figure 5: EBT-3 film response curve.

Figure 6 shows the doses measured with the four sets of application films in terms of Gy/GSF (a) and Gy/Exter.Mon. (b). Sets 1 and 2 were irradiated on day three (28 June 2017) and sets 3 and 4 on day four (29 June 2017). Both the application and calibration curve films were irradiated with the same setup as the one used for the ion chambers and alanine with a dose of approximetly 3.5 Gy. The average dose in Gy/GSF of the alanine pellets irradiated in the solid water setup is also plotted in the same figure.

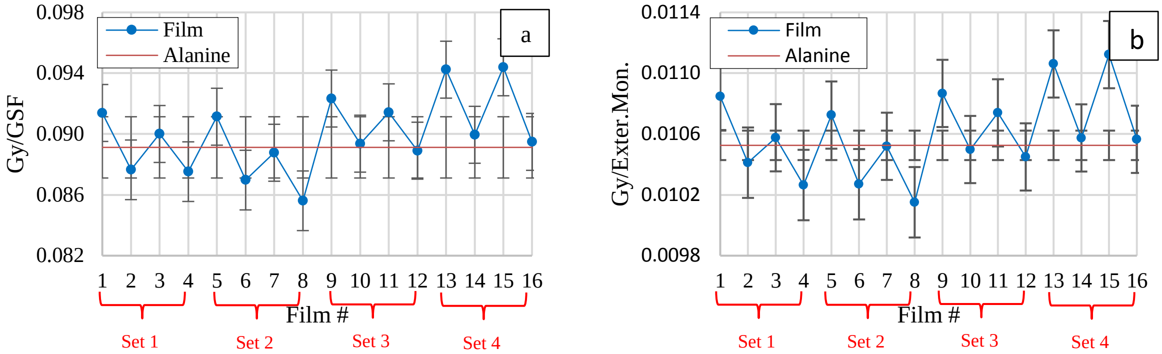

Figure 6: Dose in Gy/GSF (a) and Gy/Exter.Mon. (b) for film and alanine dosimeters in the solid water setup.

Table 10 and 11 show the statistical analysis of the film dosimetry within and between sets for Gy/GSF and Gy/Exter.Mon, respectively.

Table 10: Statistical analysis of film dosimetry within and between sets for Gy/GSF as an output.

Film set	Average dose (Gy/GSF)	SD	Relative SD	Difference from alanine
1	0.0891	1.882E-03	2.11%	0.02%
2	0.0881	2.390E-03	2.71%	-1.13%
3	0.0905	1.638E-03	1.81%	1.55%
4	0.0920	2.660E-03	2.89%	3.24%
All sets	0.0899*	2.467E-03	2.74%	0.92%

*Weighted average

Table 11: Statistical analysis of film dosimetry within and between sets Gy/Exter.Mon. as an output.

Film set	Average dose (Gy/Exter.Mon.)	SD	Relative SD	Difference from alanine
1	0.0105	2.498E-04	2.37%	-0.01%
2	0.0104	2.565E-04	2.46%	-1.04%
3	0.0106	1.981E-04	1.86%	1.07%
4	0.0108	3.024E-04	2.79%	2.90%
All sets	0.0106*	2.77E-04	2.61%	0.73%

*Weighted average

Figure 7 shows the radiation field of the Australian MRI-linac at 2.84 m distance from the target. The nominal field size was 10 cm x 10 cm at the isocentre (actual: 8.7 cm x 10 cm).

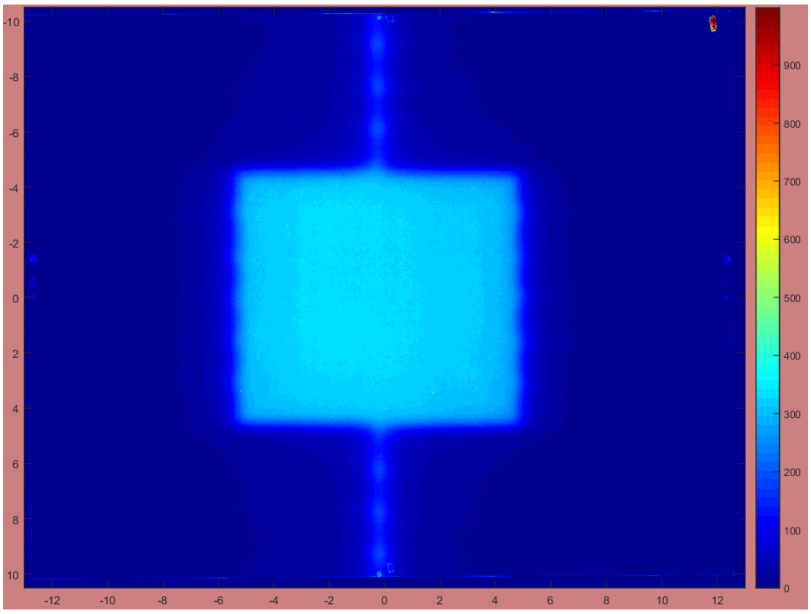

Figure 7: Radiation field of the Australian MRI-linac at 2.84 m distance from the target.

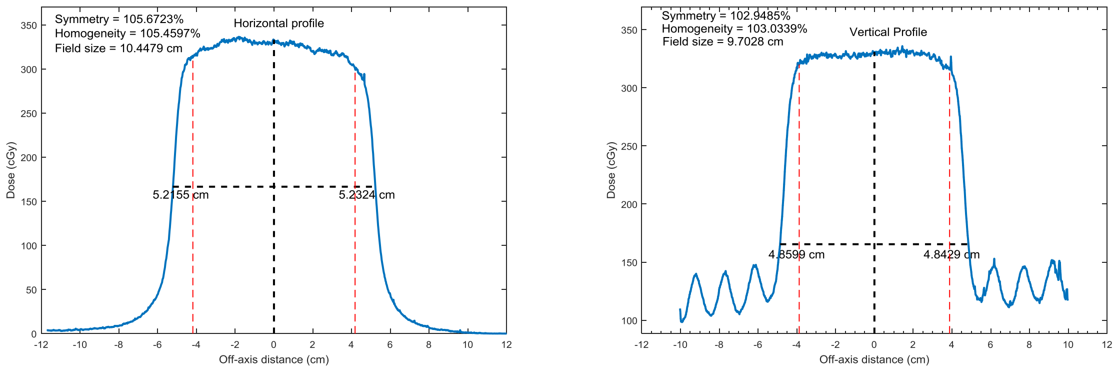

Figure 8: Horizontal and vertical profile of the radiation field of the Australian MRI-linac at 2.84 m distance from the target.

The percentage depth dose of the Australian MRI-linac is shown in figures 9 and 10. The film was placed vertically between solid water blocks. The front edge of the film was aligned with the edge of the solid water blocks and was set such that the distance between the target and the film at 10 cm depth is 2.84 m. The film was irradiated with approximetly 3.5 Gy. Figure 10a shows the percentage depth dose at approximately 25 cm and figure 10b up to a depth of 3 cm.

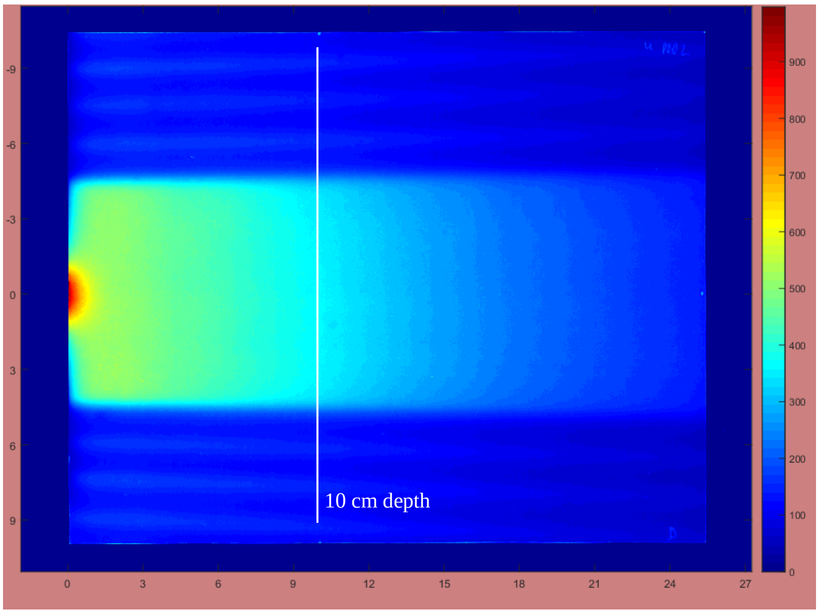

Figure 9: Image of the percentage depth dose of the Australian MRI-linac.

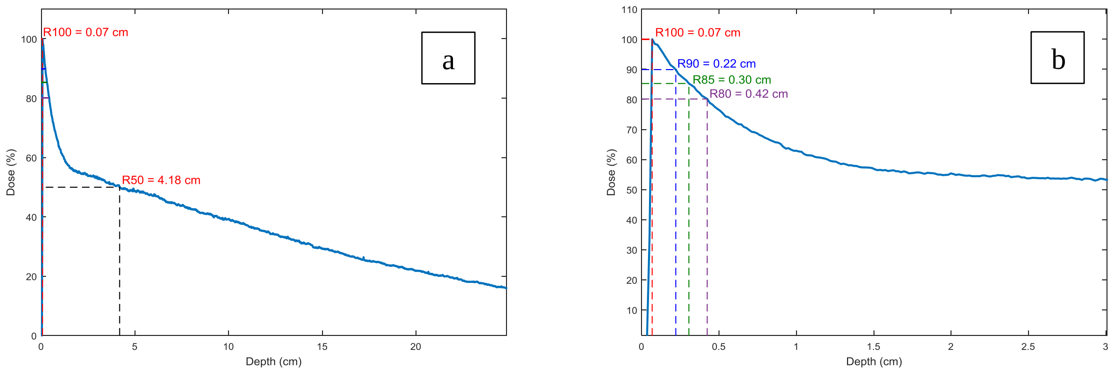

Figure 10: Percentage depth dose of the Australian MRI-linac. a) shows the depth dose up to 25 cm and b) up to 3 cm.

3.9 MEASUREMENTS AT NPL

The IBA Farmer-type chamber with s/n 819 was calibrated at NPL in both flattened and flattening filter-free beams. Further details of the measurements can be found in NPL certificates 2017RD01819-1 and 2017RD01819-2.

4 DISCUSSION

The MRI-linac beam output was calibrated using alanine dosimetry at each day and it was determined in terms of Gy/GSF and Gy/Exter.Mon. as described in section 3.2. The maximum spread of the beam output calibration determined with alanine pellets irradiated in the water tank setup was found to be 3% and 0.7% when using the MRI-linac monitor (GSF) and the external chamber (A1SL) as a monitor, respectively. It has been demonstrated that the use of an external chamber, close to the linac and far from the MRI bore, to monitor the beam, give better results compared to the MRI-linac monitoring system.

The difference between the calibration coefficients determined using the solid water and the water tank setup was found to be 0.3%.

The MRI-linac stability over a period of 3 days was examined in this work. It was found that there was a change of 0.022 nC/GSF per day if the MRI-linac monitor system is used. This translates to a maximum change in dose of 1% per day. When the external detector (A1SL) was used as a monitor chamber, the change in dose was reduced to less than 0.3% per day.

The effect of a 1 T field on the ion recombination corrections was expected to be small in accordance with previous measurements (Smit *et al.*, 2013) and the results of the measurements presented here agree with this assessment for all chamber types.

A summary of the ionisation chamber calibration coefficients (Gy/C) in terms of absorbed dose to water as measured in the Australian MRI-linac in the two different setups was presented. Calibration coefficients were relative to both the machine monitor unit (GSF) and external monitor chamber (Exter.Mon.). In all cases, the calibration coefficients of all ionisation chambers, when determined using the machine monitor, have higher values compared with calibration coefficients determined using the external monitor. The average difference is in the order of 1% with a maximum of 1.2%.

The signal of the ionisation chamber, when using the solid water setup, was compared when the 2 cm thick plate with the Farmer-shaped cavity was either filled with water or not. The difference between without and with water was found to be -0.3%.

The variation in dose from pellet to pellet within the F-type alanine holder appears to be consistent. No systematic trend was observed and the maximum variation was found to be ±0.14 Gy.

Gafchromic films were irradiated in the solid water setup. A 12-point calibration curve was generated and 16 application films (4 film pieces from 4 different film sheets) were used to obtain the dose output (in Gy/GSF). The maximum difference between dose outputs measured with the 4 set of films and alanine was found to be 3.24%. The difference between the average dose outputs of all set of films with alanine was 0.92%.

The film profiles in figure 8 suggest that the actual beam field at 2.84 m distance between the focal spot and the measurement plane is 9.7 cm x 10.4 cm. The measured beam field size is close to the 10 cm x 10 cm nominal one.

The B-field correction factor, k_Q^B, was only determined for the IBA Farmer-type chamber (s/n: 819) because it was the only detector that was calibrated at NPL in a flattening filter-free energy beam. It was found that the correction is of the order of 0.998 and 0.990 when using the MRI-linac monitor (GSF) and the external chamber (A1SL) as a monitor, respectively.

The uncertainty in the absorbed dose to water calibration coefficients, N_{Dw}, determined based on the alanine measurements at the Australian MRI-linac, is 3% and 2% when using machine monitor unit (GSF) and an external monitor chamber, respectively. Uncertainty is based on a standard uncertainty multiplied by a coverage factor $k = 2$, providing a coverage probability of approximetly 95%.

5 CONCLUSION

It is possible to carry out accurate dosimetry in the MRI-linac beam at Liverpool Hospital, Australia provided care is taken in the setup and positioning of any phantom used. Care should also be taken when the MRI-linac monitor system is used to determine dose as this could lead to an error of about 3% within three days.

Calibration coefficients for different ionisation chambers were determined using alanine dosimetry as a reference standard with an uncertainty of 2% ($k = 2$).

Radiochromic film dosimetry agrees well with alanine dosimetry when comparing beam output measurements. Unlike other air-filled detectors, radiochromic film is not strongly affected by the

B-field. A study at NPL has shown that the influence of the B-field strength on the radiochromic film sensitivity has a weak effect (typically in the order of 1.5% per T). Nevertheless, the best overall uncertainty achievable in dosimetry using radiochromic EBT-3 film, ranging from 1% to 2% (Bouchard *et al.*, 2009, Martisikova *et al.*, 2008), this remains a promising dosimeter for absolute and relative dosimetry in MRI-guided radiotherapy.

In order to complete reference dosimetry measurements using ionisation chambers, a correction is required for the effect of the B-field strength. It is possible to calculate this correction by using alanine as a reference detector.

6 ACKNOWLEDGEMENTS

The authors acknowledge people from Ingham Institute in Liverpool, New South Wales, Australia for access to the Australian MRI-linac. They would also like to gratefully acknowledge Jarrad Begg, Urszula Jelen, Bin Dong from Liverpool Cancer Therapy Centre for their help with the measurements and Thorsten Sander from NPL for his useful comments on the report.

7 REFERENCES

Bouchard, H., Lacroix, F., Beaudoin, G., Carrier, J. F. & Kawrakow, I. 2009. On the characterization and uncertainty analysis of radiochromic film dosimetry. *Medical Physics,* 36**,** 1931-1946.

Gallas, R. Towards alanine/ESR as a secondary standard for dosimetry in magnetic fields. 5th MR in RT Symposium, 2017 Sydney, Australia.

Keall, P. J., Barton, M., Crozier, S. & Australian, M. R. I. L. P. 2014. The Australian Magnetic Resonance Imaging-Linac Program. *Seminars in Radiation Oncology,* 24**,** 203-206.

Liney, G. P., Dong, B., Begg, J., Vial, P., Zhang, K., Lee, F., Walker, A., Rai, R., Causer, T., Alnaghy, S. J., Oborn, B. M., Holloway, L., Metcalfe, P., Barton, M., Crozier, S. & Keall, P. 2016. Technical Note: Experimental results from a prototype high-field inline MRI-linac. *Medical Physics,* 43**,** 5188-5194.

Martisikova, M., Ackermann, B. & Jakel, O. 2008. Analysis of uncertainties in Gafchromic (R) EBT film dosimetry of photon beams. *Physics in Medicine and Biology,* 53**,** 7013-7027.

Meijsing, I., Raaymakers, B. W., Raaijmakers, A. J. E., Kok, J. G. M., Hogeweg, L., Liu, B. & Lagendijk, J. J. W. 2009. Dosimetry for the MRI accelerator: the impact of a magnetic field on the response of a Farmer NE2571 ionization chamber. *Physics in Medicine and Biology,* 54**,** 2993-3002.

O'Brien, D. J., Roberts, D. A., Ibbott, G. S. & Sawakuchi, G. O. 2016. Reference dosimetry in magnetic fields: formalism and ionization chamber correction factors. *Medical Physics,* 43**,** 4915-4927.

Raaijmakers, A. J. E., Raaymakers, B. W. & Lagendijk, J. J. W. 2005. Integrating a MRI scanner with a 6 MV radiotherapy accelerator: dose increase at tissue-air interfaces in a lateral magnetic field due to returning electrons. *Physics in Medicine and Biology,* 50**,** 1363-1376.

Raaijmakers, A. J. E., Raaymakers, B. W., van der Meer, S. & Lagendijk, J. J. W. 2007. Integrating a MRI scanner with a 6 MV radiotherapy accelerator: impact of the surface orientation on the entrance and exit dose due to the transverse magnetic field. *Physics in Medicine and Biology,* 52**,** 929-939.

Raaymakers, B. W., Raaijmakers, A. J. E., Kotte, A., Jette, D. & Lagendijk, J. J. W. 2004. Integrating a MRI scanner with a 6 MV radiotherapy accelerator: dose deposition in a transverse magnetic field. *Physics in Medicine and Biology,* 49**,** 4109-4118.

Reynolds, M., Fallone, B. G. & Rathee, S. 2013. Dose response of selected ion chambers in applied homogeneous transverse and longitudinal magnetic fields. *Medical Physics,* 40**,** 7.

Saur, S. & Frengen, J. 2008. GafChromic EBT film dosimetry with flatbed CCD scanner: A novel background correction method and full dose uncertainty analysis. *Medical Physics,* 35**,** 3094-3101.

Smit, K., van Asselen, B., Kok, J. G. M., Aalbers, A. H. L., Lagendijk, J. J. W. & Raaymakers, B. W. 2013. Towards reference dosimetry for the MR-linac: magnetic field correction of the ionization chamber reading. *Physics in Medicine and Biology,* 58**,** 5945-5957.

Spindeldreier, C. K., Schrenk, O., Bakenecker, A., Kawrakow, I., Burigo, L., Karger, C. P., Greilich, S. & Pfaffenberger, A. 2017. Radiation dosimetry in magnetic fields with Farmer-type ionization chambers: determination of magnetic field correction factors for different magnetic field strengths and field orientations. *Physics in Medicine and Biology,* 62**,** 6708-6728.